A Comparative Power Quality Study of DFIG and PMSG Based Wind Energy Conversion System

LATA GIDWANI
Department of Electrical Engineering
Rajasthan Technical University
Rawatbhata Road, Kota, Rajasthan
INDIA
lata_gidwani@rediffmail.com

Abstract: - Wind Energy Generation Systems (WECS) are confronted with increasing demands for power quality and harmonic distortion control. With the advances in power electronics technology, the rapid growth of variable speed WECS is now witnessed. However, the power quality still remains an important issue to be addressed thoroughly by researchers. This paper presents a comparative study on grid connected WECS having two different Wind Turbine Generator Systems (WTGS) using DFIG and PMSG. Both WTGS systems are connected to power grid through conventional back to back converters and Unconventional Power Electronic Interface (UPEI) in different cases. Four cases are compared examining the effect of proposed unconventional power electronic interface on both WTGS systems. Transient simulations are carried out under the condition of sudden short circuit disturbance and the performance of both systems is compared for active power, reactive power and speed control. The comparison also aims to present in a thorough and coherent way the aspects of power quality in terms of reduction in Total Harmonic Distortion (THD) at various fault locations and buses. All the simulations are made in Matlab/Simulink.

Key-Words: - Wind Energy Conversion System, Wind Turbine Generator System, Unconventional Power Electronic Interface, Power Quality, Total Harmonic distortion.

1 Introduction

Wind Energy Conversion Systems (WECS) constitute a mainstream power technology that is largely under exploited. At present, typically two types of WECS for large wind turbines exists [1-3]. The first one is a variable speed WECS using Doubly Fed Induction Generator (DFIG) that allows variable speed operation over a large, but still restricted, range. This type of WECS offer high controllability, smoother grid connection, maximum power extraction and reactive power compensation using back to back power converters of rating near to 25-30% of the generator capacity [2-4]. The second one is also a variable speed WECS using Permanent Magnet Synchronous Generator (PMSG). With PMSG the gear box can be eliminated by using large number of poles that allows higher efficiency. With large-scale exploration and integration of wind sources, variable speed wind turbine generators, PMSG [5-6] are emerging as the preferred technology. The complete modeling and simulation of a grid interfaced WECS based on DFIG, using dynamic vector approach is presented in [7-9]. In [10-12], control schemes for grid connected WECS using PMSG are presented.

In the present work, a WECS has been modeled and simulated for the following two WTGS configurations: (i) using DFIG and (ii) using PMSG with conventional or unconventional power electronic interface. The performances of both DFIG and PMSG based WECS have been compared in terms of power quality, active power, reactive power and speed control. Four cases are considered showing comparison of conventional back to back converter and unconventional power electronic interface in both WTGS systems. The paper is organized as follows: Section 1 presents an introduction along with objectives of the present work. System configuration and proposed strategy for four cases are described in Section 2. The simulation models developed in MATLAB Simulink are detailed in Section 2 and the results obtained from these models are explained and compared in Section 3. The conclusions drawn from these results are finally summarized in Section 4.

2 System Description

Four different cases are considered here examining the effect of conventional back to back converter and unconventional power electronic interface on DFIG and PMSG as wind turbine generators. The design parameters of wind turbine are shown in Table 1.

Table 1
Design Parameters of Wind Turbine

Quantity	Wind Turbine Data for One Wind Turbine
Nominal turbine mechanical power	3 MW
base wind speed	9 m/sec.
pitch angle controller integral gain	5
pitch angle controller proportional gain	25
maximum pitch angle	45 deg.
maximum rate of change of pitch angle	2deg./sec

2.1 Case 1: Wind Energy Conversion System using DFIG with Conventional Back to Back Converters

This section considers the mutual effects of integrating wind power using DFIG with conventional back to back converters in power systems under transient fault situations. A 9 MW wind-farm consisting of three 3 MW wind turbines, connected to a 33 kV distribution system, exports power to a 220 kV grid through a 30 km, 33 kV feeder. A 500 KW resistive load and a 0.9 MVAR (Q = 50) filter are connected at the 440 V bus. A fault is simulated and connected to 132 kV line and grounding transformer is connected to 33 kV bus. Fig.1 shows the layout of the wind system with its interconnection to the transmission grid.

When DFIG is a wound rotor machine where the rotor circuit is connected to an external variable voltage and frequency source via slip rings and the stator is connected to the grid network [13, 15]. There is also a possibility of altering the rotor reactance by effectively modulating some inductors in series with the original rotor reactance. While modeling DFIG, the generator convention will be used, which means that the currents are outputs instead of inputs and real power and reactive power have a positive sign when they are fed into the grid.

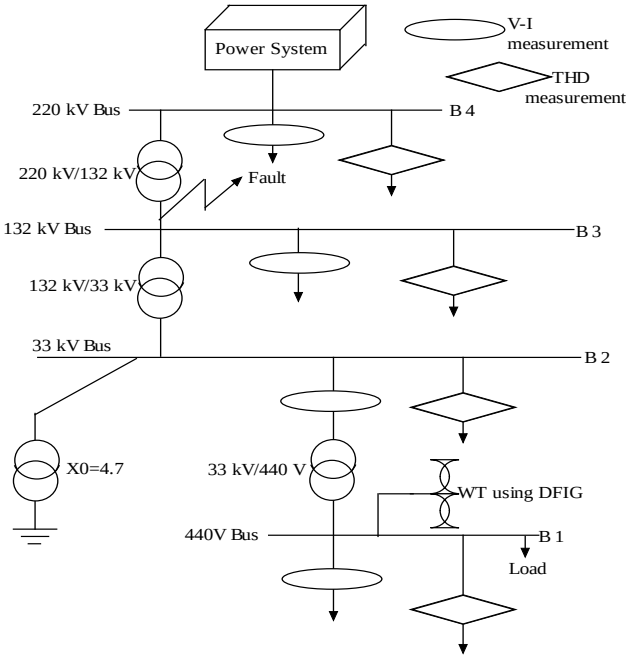

Fig.1: Power System Model Integrated with Wind Power using DFIG

Using the generator convention, the following equations results,

$$v_{ds} = -R_s i_{ds} - \omega_s \varphi_{qs} + \frac{d}{dt}\varphi_{ds} \quad (1)$$

$$v_{qs} = -R_s i_{qs} + \omega_s \varphi_{ds} + \frac{d}{dt}\varphi_{qs} \quad (2)$$

$$v_{dr} = -R_r i_{dr} - s\omega_s \varphi_{qr} + \frac{d}{dt}\varphi_{dr} \quad (3)$$

$$v_{qr} = -R_r i_{qr} + s\omega_s \varphi_{dr} + \frac{d}{dt}\varphi_{qr} \quad (4)$$

where,
v_{ds}, i_{ds} :d-Axis Stator Voltage and Current respectively
v_{qs}, i_{qs} :q-Axis Stator Voltage and Current respectively
v_{dr}, i_{dr} :d-Axis Rotor Voltage and Current respectively
v_{qr}, i_{qr} :q-Axis Rotor Voltage and Current respectively
R_s : Stator Resistance
R_r : Rotor Resistance
φ_{qs} : q-Axis Stator Flux Linkage
φ_{ds} : d-Axis Stator Flux Linkage
φ_{qr} : q-Axis Rotor Flux Linkage
φ_{dr} : d-Axis Rotor Flux Linkage
ω_s : Stator Electrical Frequency
s :Rotor Slip

The d-q reference frame is rotating at synchronous speed with the q-axis 90° ahead of the d-axis. The position of the d-axis coincides with the maximum of the stator flux, which means that v_{qs} equals the terminal voltage and v_{ds} equals zero. The flux linkages can be calculated using the following set of equations in per unit:

$$\varphi_{ds} = -(L_s + L_m)\, i_{ds} - L_m\, i_{dr} \quad (5)$$

$$\varphi_{qs} = -(L_s + L_m)\, i_{qs} - L_m\, i_{qr} \quad (6)$$

$$\varphi_{dr} = -(L_r + L_m)\, i_{dr} - L_m\, i_{ds} \quad (7)$$

$$\varphi_{qr} = -(L_r + L_m)\, i_{qr} - L_m\, i_{qs} \quad (8)$$

where L_s and L_r are stator and rotor leakage inductance respectively and L_m is the mutual inductance between the stator and the rotor. The rotor slip s is defined as:

$$s = \frac{\omega_s - \frac{p}{2}\omega_m}{\omega_s} \quad (9)$$

where p is the pairs of poles and ω_m is the mechanical frequency of the generator. The active power P and reactive power Q generated by the DFIG:

$$P = v_{ds} i_{ds} + v_{qs} i_{qs} + v_{dr} i_{dr} + v_{qr} i_{qr} \quad (10)$$

$$Q = v_{qs} i_{ds} - v_{ds} i_{qs} + v_{qr} i_{dr} - v_{dr} i_{qr} \quad (11)$$

However, also the mechanical part should be taken into account in developing a dynamic model. The following equation gives electromechanical torque T_e generated by the DFIG:

$$T_e = \varphi_{dr}\, i_{qr} - \varphi_{qr}\, i_{dr} \quad (12)$$

The changes in generator speed that result from a difference in electrical and mechanical torque can be calculated as:

$$\frac{d\omega}{dt} = \frac{1}{2H}\left(T_m - T_e\right) \quad (13)$$

where H is the inertia constant and T_m is the mechanical torque. The design parameters of DFIG are shown in Table 2.

Table 2
Generator Parameters of Wind Turbine

Quantity	Generator Data
nominal electrical power	3.33 MVA
stator resistance, r_s	0.023 p.u.
stator inductance, l_s	0.18 p.u.
rotor resistance, r_r	0.016 p.u.
rotor inductance, l_r	0.16 p.u.
magnetizing inductance, l_m	2.9 p.u.
inertia constant, h	0. 685
pairs of poles, p	3

The WECS considered for analysis consist of a DFIG driven by a wind turbine, rotor side converter and grid side converter, as shown in Fig.2.

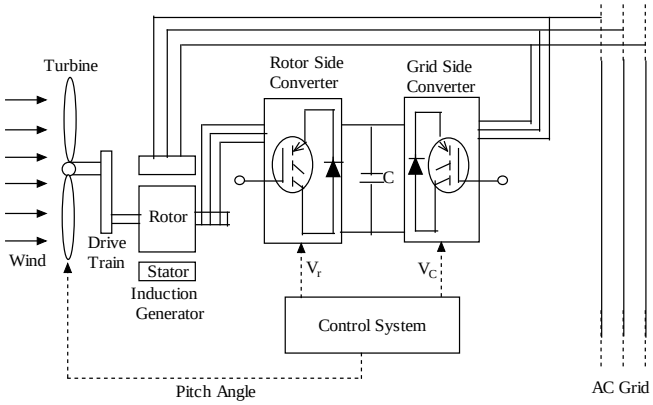

Fig.2: Wind Energy Conversion System with DFIG and Conventional Converters

Rotor side converter consists of three phase IGBT-Diode rectifier connected in Graetz bridge configuration with snubber resistance and capacitance. The circuit is discretized at a sample time of 2 μs. Grid side converter also consists of three phase IGBT-Diode rectifier connected in Graetz bridge configuration. The grid side converter is used to regulate the voltage of the DC bus capacitor.

The pitch angle control is used to limit the power extracted at high wind speeds conditions. The control system uses a torque controller in order to maintain the speed. The reactive power produced by the wind turbine is also regulated at zero MVAR.

2.2 Case 2: Wind Energy Conversion System using DFIG with Unconventional Power Electronic Interface

The WECS considered for analysis consist of a DFIG driven by a wind turbine, rotor side converter, DC to DC intermediate circuit and grid side converter [16]. Fig.3 shows a schematic diagram of WECS having DFIG and UPEI that will be discussed in this paper.

Rotor side converter consists of three-phase IGBT-diode rectifier connected in Graetz bridge configuration with snubber resistance and capacitance. The circuit is discretized at a sample time of 2 μs. Fig.4 shows voltage and VAR regulation of rotor side converter and regulators of converter 1 are shown in Fig.5. The pitch angle is regulated at zero degree by pitch angle regulator until the speed w_r reaches desired speed of the tracking characteristic w_d. Beyond w_d, the pitch angle is proportional to the speed deviation from desired speed. The control system is illustrated in the Fig.6. The WECS having UPEI is connected to a 33 kV distribution system exports power to a 220 kV grid as shown in Fig.7. A transient fault at t=0.104 s for a duration of 3 ms is simulated at B3. The control system is used to maintain the speed at 1 pu and to regulate reactive power produced by the wind turbine at zero MVAR.

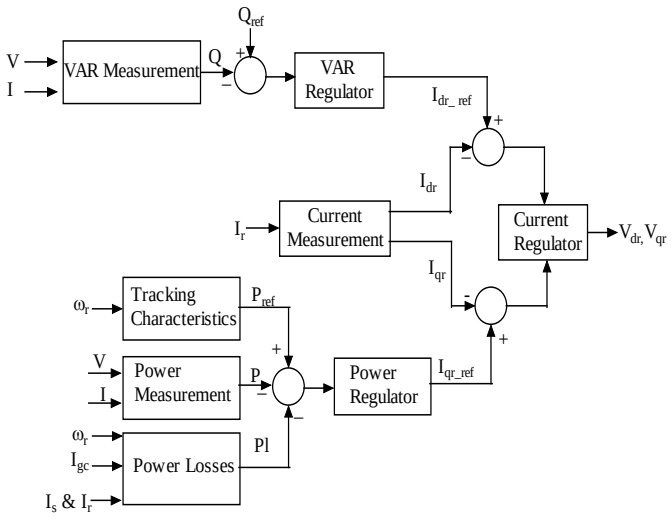

Fig.4: Voltage and VAR Regulator of Rotor Side Converter

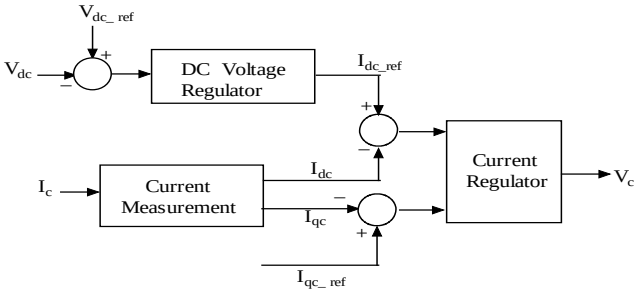

Fig.5: Voltage and Current Regulator of Converter1

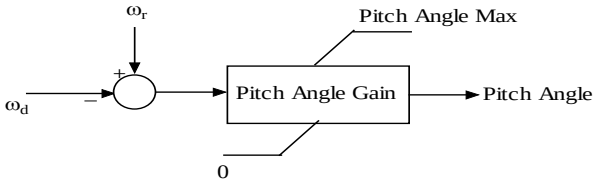

Fig.6: Pitch Control System.

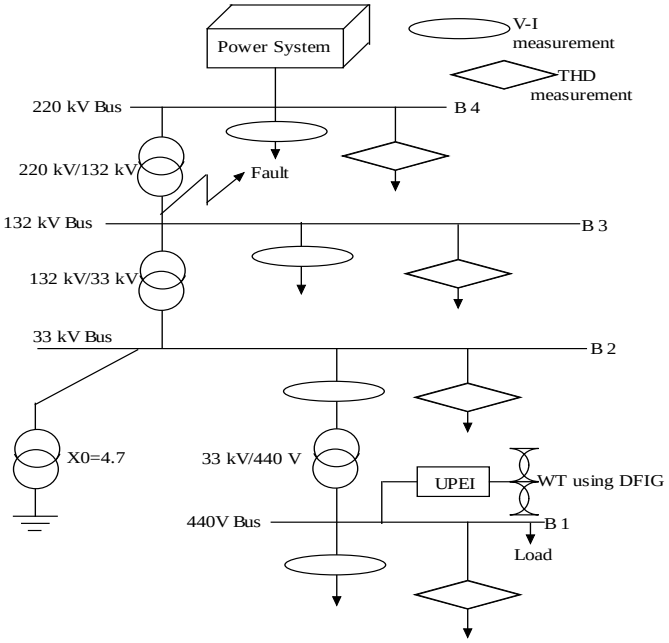

Fig.7: Power System Model used in Case 2

2.3 Case 3: Wind Energy Conversion System using PMSG with Conventional Back to Back Converters

The WECS considered for analysis consist of a PMSG driven by a wind turbine connected to power grid using conventional back to back converters. The modeling of WECS remains same except DFIG is replaced with PMSG. Thus only modeling of PMSG will be discussed here and remaining model is same as that of Case 1. The electrical model of PMSG [11-12] in the synchronous reference frame is given in literature [17-19]. The design parameters of PMSG are shown in Table 3. Following are the

equations used in modeling of PMSG:

$$V_d = R_s i_d + \frac{d}{dt}\varphi_d - \omega_r \varphi_q \quad (14)$$

$$V_q = R_s i_q + \frac{d}{dt}\varphi_q + \omega_r \varphi_d \quad (15)$$

$$V'_{fd} = R'_{fd} i'_{fd} + \frac{d}{dt}\varphi'_{fd} \quad (16)$$

$$V'_{kd} = R'_{kd} i'_{kd} + \frac{d}{dt}\varphi'_{kd} \quad (17)$$

$$V'_{kq1} = R'_{kq1} i'_{kq1} + \frac{d}{dt}\varphi'_{kq1} \quad (18)$$

$$V'_{kq2} = R'_{kq2} i'_{kq2} + \frac{d}{dt}\varphi'_{kq2} \quad (19)$$

$$\varphi_d = L_d i_d + L_{md}\,(i'_{fd} + i'_{kd}) \quad (20)$$

$$\varphi_q = L_q i_q + L_{mq}\, i'_{kq} \quad (21)$$

$$\varphi'_{fd} = L'_{fd} i'_{fd} + L_{md}\,(i_d + i'_{kd}) \quad (22)$$

$$\varphi'_{kd} = L'_{kd} i'_{kd} + L_{md}\,(i_d + i'_{fd}) \quad (23)$$

$$\varphi'_{kq1} = L'_{kq1} i'_{kq1} + L_{mq}\, i_q \quad (24)$$

$$\varphi'_{kq2} = L'_{kq2} i'_{kq2} + L_{mq}\, i_q \quad (25)$$

$$T_e = \varphi_d i_q + \varphi_q\, i_d \quad (26)$$

where
V_q, V_d:q-Axis and d-Axis Voltages respectively
R_s:Resistance of the Stator Windings
i_q, i_d:q-Axis and d-Axis Currents respectively
φ_q, φ_d:q-Axis and d-Axis Fluxes respectively
ω_r:Angular Velocity of the Rotor
V'_{fd} , V'_{kd}:d-Axis Field and Damper Winding Voltage
R'_{fd} , R'_{kd} :d-Axis Field Winding and Damper Winding Resistance respectively
i'_{fd} , i'_{kd}:d-Axis Field Winding and Damper Winding Current respectively
φ'_{fd} , φ'_{kd}:d-Axis Field Winding and Damper Winding Flux respectively
L'_{fd} , L'_{kd}:d-Axis Field Winding and Damper Winding Inductance respectively
V'_{kq1} , V'_{kq2}:q-Axis Damper Winding O/P Voltage 1 and Voltage 2 respectively
R'_{kq1} , R'_{kq2}:q-Axis Damper Winding O/P Resistance 1 and 2 respectively
i'_{kq1} , i'_{kq2}:q-Axis Damper Winding O/P Current 1 and Current 2 respectively
φ'_{kq1} , φ'_{kq2}:q-Axis Damper Winding O/P Flux 1 and Flux 2 respectively
L'_{kq1} , L'_{kq2}:q-Axis Damper Winding O/P Circuit Inductance 1 and 2 respectively
L_q, L_d:q-Axis and d-Axis Inductances respectively
L_{mq}, L_{md}:q-Axis and d-Axis Magnetizing Inductances respectively
T_e:Electromagnetic Torque

Mechanical system for the model is :

$$\frac{d\omega_r}{dt} = \frac{T_e - F\omega_r - T_m}{J} \quad (27)$$

$$\frac{d\theta}{dt} = \omega_r \quad (28)$$

where,
J :Combined Inertia of Rotor and Load
F : Combined Viscous Friction of Rotor and Load
θ :Rotor Angular Position
T_m: Shaft Mechanical Torque

Table 3
Design Parameters of PMSG

Quantity	PMSG Data
nominal electrical power	3.33 MVA
nominal frequency	50 Hz
d-axis inductance, l_d	0.00415 p.u.
q-axis inductance, l_q	0.0015 p.u.
stator resistance, r_s	0.006 p.u.
friction factor, f	0.01 p.u.

2.4 Case 4: Wind Energy Conversion System using PMSG with Unconventional Power Electronic Interface

The WECS considered for analysis consist of a PMSG driven by a wind turbine, three phase rectifier, an intermediate DC circuit and a PWM inverter. The WECS using PMSG with UPEI [16] is shown in Fig.8.

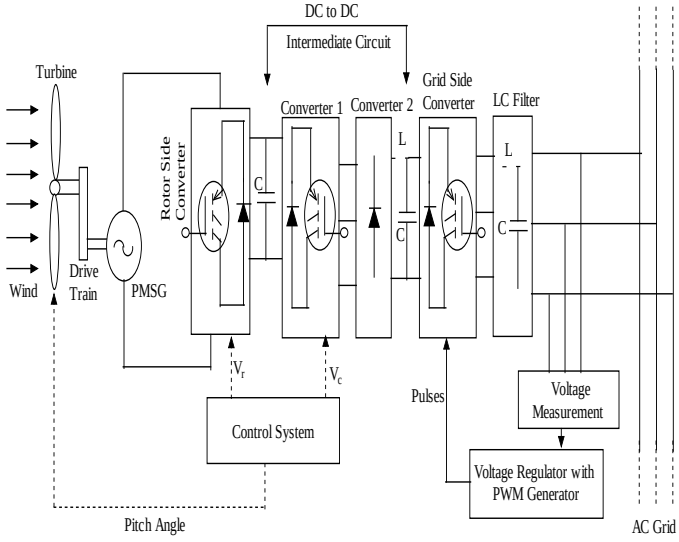

Fig.8: Case 4: Wind Energy Conversion System with PMSG and Controlled Unconventional Power Electronic Interface

3 Comparison of Different Cases

The induction generators that are used in the wind turbine are usually SCIG, DFIG and in nowadays PMSG. Currently, DFIG based wind turbines dominate the world market due to variable-speed operation, as well as the controlling flexibility of reactive power. DFIG has almost replaced SCIG as a wind generator. PMSG is emerging as new generator for wind turbine nowadays. This section presents a comparative study of PMSG and DFIG. The comparison of active and reactive power of DFIG and PMSG is shown in Fig.9 and Fig.10 respectively. The comparison of DFIG and PMSG rotor speed is shown in Fig.11.

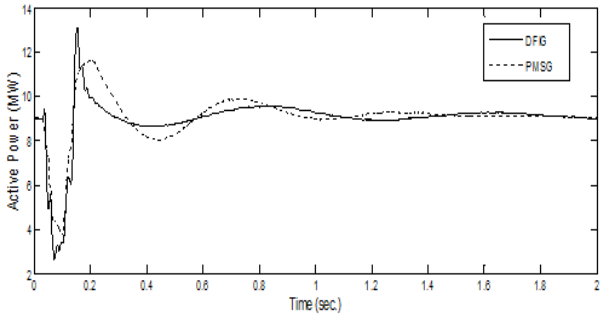

Fig.9: Active Power Comparison of DFIG and PMSG

The oscillations in active power of PMSG are less than that of DFIG during fault. Both PMSG and DFIG take approximately same time to reach steady-state value of 9 MW.

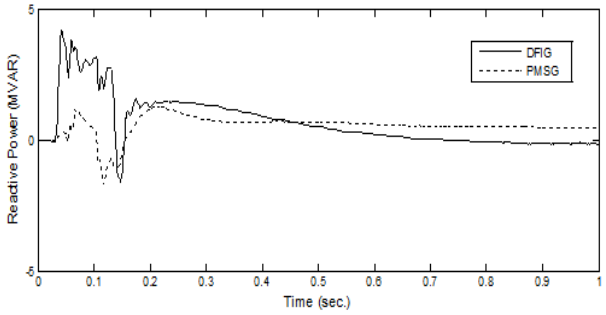

Fig.10: Reactive Power Comparison of DFIG and PMSG

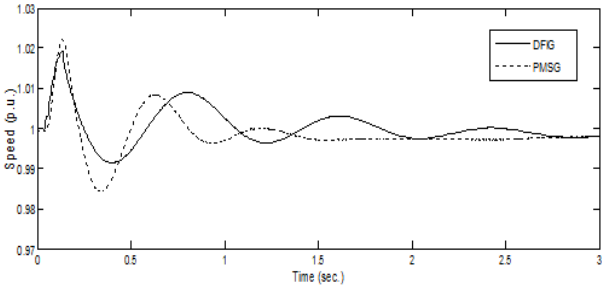

Fig.11: Generator Rotor Speed Comparison of DFIG and PMSG

As clear from Fig.10, reactive power regulation of PMSG at zero MVAR is much better than DFIG during fault. The deviation of reactive power from zero MVAR is much less in PMSG than DFIG during fault, but after fault clearance, reactive power of DFIG returns to zero value in much less time than PMSG. So, if system needs that reactive power should not be deviated much from zero MVAR, then PMSG could be better choice and if system needs that reactive power should be regulated at zero MVAR more time and sudden high deviations are allowed, then DFIG could be better choice. The comparison of DFIG and PMSG rotor speed is shown in Fig.11. The speed of PMSG reaches its steady-state value in comparatively much lesser time than DFIG. The steady-state value of PMSG is reached at t = 1.5 seconds and DFIG oscillates even at t = 3 seconds. Hence if speed regulation is of more importance, then PMSG should be the choice. The values of THDs during different faults and at various fault locations during cases 1 to 4 are shown in Table 4 to Table 7.

THD measured at different buses during unsymmetrical and symmetrical faults and at different fault locations during Case 1 is shown in Table 4. The harmonic distortion is maximum when single phase fault occurs at bus B3 and THD is measured at bus B1. The harmonic distortion is minimum when THD is measured at bus B4 and two phase fault occurs at bus B1. It is observed that THD measured at bus B1 is same when fault occurs

at bus B4 irrespective of type of fault. The same is true when THD is measured at buses B2 to B4. THD is more when measured at Bus B1, decreases as bus voltages increase, becoming minimum when measured at Bus B4.

Table 5 shows THD measured at different buses during unsymmetrical and symmetrical faults and at different fault locations during Case 2. It is seen that THD measured at different buses reduces for all types of fault in Case 2 as compared to Case 1. The reduction in THD measured at different buses in Case 2 as compared to Case 1 ranges from 40% to 60% (approx.) for different faults and fault locations.

TABLE 4
CASE 1: WIND ENERGY CONVERSION USING DFIG WITH CONVENTIONAL BACK TO BACK CONVERTERS

Fault Location	THD Measured (% of Fundamental) at Bus B1						THD Measured (% of Fundamental) at Bus B2					
	1φ	1φG	2φ	2φG	3φ	3φG	1φ	1φG	2φ	2φG	3φ	3φG
Bus B1	9.94	9.4	7.68	7.79	6.39	6.69	5.27	5.29	5.28	5.42	4.93	5.02
Bus B2	9.8	8.96	7.68	7.68	7.42	7.42	5.1	5.4	8.18	7.59	7.33	7.33
Bus B3	10.52	9.76	7.94	8.9	9.76	7.24	5.46	6.26	5.32	5.62	6.26	5.7
Bus B4	9.89	9.89	9.89	9.89	9.89	9.89	5.32	5.32	5.32	5.32	5.32	5.32
Fault Location	THD Measured (% of Fundamental) at Bus B3						THD Measured (% of Fundamental) at Bus B4					
Bus B1	2.31	2.34	2.94	3.03	3.39	3.36	0.11	0.09	0.08	0.07	0.13	0.11
Bus B2	2.19	2.72	7.68	7.45	7.31	7.31	0.09	0.1	0.28	0.29	0.3	0.3
Bus B3	2.8	4.08	3.79	4.1	4.06	4.51	0.14	0.18	0.17	0.19	0.18	0.19
Bus B4	2.29	2.29	2.29	2.29	2.29	2.29	0.1	0.1	0.1	0.1	0.1	0.1

TABLE 5
CASE 2: WIND ENERGY CONVERSION USING PMSG WITH CONVENTIONAL BACK TO BACK CONVERTERS

Fault Location	THD Measured (% of Fundamental) at Bus B1						THD Measured (% of Fundamental) at Bus B2					
	1φ	1φG	2φ	2φG	3φ	3φG	1φ	1φG	2φ	2φG	3φ	3φG
Bus B1	3.18	3.66	1.96	2.18	2.2	2.09	4.46	4.78	4.21	4.27	4.07	4.12
Bus B2	3.35	2.67	5.73	5.11	3.77	3.58	4.06	4.23	6.31	5.93	5.61	4.05
Bus B3	1.92	1.72	2.52	1.49	2.53	1.51	3.95	3.86	4.52	3.85	4.28	3.87
Bus B4	3.18	3.18	3.18	3.18	3.18	3.18	4.46	4.46	4.46	4.46	4.46	4.46
Fault Location	THD Measured (% of Fundamental) at Bus B3						THD Measured (% of Fundamental) at Bus B4					
Bus B1	1.3	1.66	1.44	1.48	1.42	1.73	0.06	0.06	0.06	0.07	0.13	0.09
Bus B2	1.29	2.67	4.18	4.11	4.39	1.47	0.05	0.12	0.11	0.13	0.3	0.12
Bus B3	0.61	0.98	2.14	2.05	1.3	1.35	0.05	0.08	0.21	0.13	0.18	0.15
Bus B4	1.3	1.3	1.3	1.3	1.3	1.3	0.06	0.06	0.06	0.06	0.06	0.06

TABLE 6
CASE 3: WIND ENERGY CONVERSION USING DFIG WITH UNCONVENTIONAL POWER ELECTRONIC INTERFACE

Fault Location	THD Measured (% of Fundamental) at Bus B1						THD Measured (% of Fundamental) at Bus B2					
	1φ	1φG	2φ	2φG	3φ	3φG	1φ	1φG	2φ	2φG	3φ	3φG
Bus B1	1.44	1.44	1.57	1.58	1.2	1.15	0.28	0.28	0.27	0.27	0.28	0.28
Bus B2	1.44	1.53	1.46	1.91	1.63	2.06	0.28	0.27	0.27	0.29	0.26	0.29
Bus B3	1.49	2.18	2.15	2.08	2.03	2.1	0.28	0.33	0.32	0.31	0.32	0.33
Bus B4	1.44	1.44	1.44	1.44	1.44	1.44	0.28	0.28	0.28	0.28	0.28	0.28
Fault Location	THD Measured (% of Fundamental) at Bus B3						THD Measured (% of Fundamental) at Bus B4					
Bus B1	0.26	0.26	0.25	0.25	0.28	0.28	0.01	0.01	0.01	0.01	0.01	0.01
Bus B2	0.26	0.25	0.25	0.3	0.25	0.3	0.01	0.01	0.02	0.02	0.02	0.02
Bus B3	0.26	0.33	0.34	0.34	0.34	0.35	0.01	0.01	0.01	0.01	0.01	0.02
Bus B4	0.26	0.26	0.26	0.26	0.26	0.26	0.01	0.01	0.01	0.01	0.01	0.01

TABLE 7
CASE 4: WIND ENERGY CONVERSION USING PMSG WITH UNCONVENTIONAL POWER ELECTRONIC INTERFACE

Fault Location	THD Measured (% of Fundamental) at Bus B1						THD Measured (% of Fundamental) at Bus B2					
	1φ	1φG	2φ	2φG	3φ	3φG	1φ	1φG	2φ	2φG	3φ	3φG
Bus B1	0.66	0.66	0.67	0.67	0.62	0.62	0.27	0.27	0.26	0.26	0.27	0.27
Bus B2	0.66	0.68	0.65	0.68	0.76	0.76	0.27	0.26	0.26	0.26	0.26	0.28
Bus B3	0.67	0.7	0.68	0.68	0.81	0.82	0.27	0.32	0.31	0.31	0.32	0.32
Bus B4	0.66	0.66	0.66	0.66	0.66	0.66	0.27	0.27	0.27	0.27	0.27	0.27
Fault Location	THD Measured (% of Fundamental) at Bus B3						THD Measured (% of Fundamental) at Bus B4					
Bus B1	0.25	0.25	0.25	0.25	0.28	0.28	0.01	0.01	0.01	0.01	0.01	0.01
Bus B2	0.25	0.25	0.25	0.25	0.25	0.29	0.01	0.01	0.01	0.02	0.02	0.02
Bus B3	0.25	0.32	0.33	0.33	0.34	0.34	0.01	0.01	0.01	0.01	0.01	0.01
Bus B4	0.25	0.25	0.25	0.25	0.25	0.25	0.01	0.01	0.01	0.01	0.01	0.01

THD measured at different buses during unsymmetrical and symmetrical faults and at different fault locations during Case 3 is shown in Table 6. The reduction in THD measured at different buses in Case 3 as compared to Case 1 for all types of faults and different fault locations are more than 80% approx. Thus it is concluded that THD reduces drastically when an unconventional power electronic interface is added between wind turbines using DFIG as generator in place of conventional back to back converter. This proves effectiveness of unconventional power electronic interface in wind energy conversion system using DFIG as generator.

Table 7 shows THD measured at different buses during unsymmetrical and symmetrical faults and at

different fault locations during Case 4. It is observed that THD reduces most in comparison to all the other cases. The reduction in THD measured at different buses is more than 80% as compared to Case 2, where conventional back to back converters are used as power electronic interface. Also the THD values in Case 4 are less than THD values in Case 3. Hence Case 4 is most effective case and THD values are least in this case. So, harmonic distortion is least and power quality is best in Case 4. Thus it is concluded that PMSG is more effective as compared to DFIG as wind turbine generator and also unconventional power electronic interface is more effective as an interface than conventional power electronic interface.

4 Conclusion

An attempt has been made in this paper to compare the performances of the WECS based on DFIG and PMSG, pertaining to power quality, active power, reactive power and speed control that each of the generators can handle. The system models are developed in the MATLAB/Simulink. This paper has presented the detailed model of the variable speed wind turbine with DFIG and PMSG connected to power grid through conventional or unconventional power electronic interface simulated as different cases. At the same time, the paper addresses control schemes of the wind turbine in terms of pitch angle control, AC and DC voltage regulation, VAR regulation and current regulation of converter systems. Four different cases are considered and results obtained are compared. The comparison results show that one can choose any of PMSG or DFIG as wind generator according to need. It is observed that Case 4, WECS using PMSG connected to grid through unconventional power electronic interface is most efficient in terms of power quality. As a whole, it can be concluded that the wind energy conversion system using PMSG as wind turbine generator with unconventional power electronic interface is best among all the four different cases.

References:

[1] H Li, Z Chen, "Overview of Different Wind Generator Systems and Their Comparisons", *IET Renewable Power Generation*, Vol. 2, No. 2, 2008, pp. 123-138.

[2] D. Rajib, V.T. Ranganathan, "Variable Speed Wind Power Generation Using Doubly Fed Wound Rotor Induction Machine - A Comparison with Alternative Schemes," *IEEE Transactions on Energy Conversion*, Vol. 17, No. 3, 2002, pp. 414-421.

[3] O. Carranza1, G. Garcerá, E. Figueres, L.G. González, "Low Power Wind Energy Conversion System Based on Variable Speed Permanent Magnet Synchronous Generators" *Wind Energy*, Wiley Publishers, 2013, doi: 10.1002/we.1598.

[4] F.A. Ramirez, M.A. Arjona, "Development of a Grid-Connected Wind Generation System with a Modified PLL Structure", *IEEE Transactions on Sustainable Energy*, Vol. 3, Issue 3, 2012, pp. 474 – 481.

[5] R.J. Wai, C.Y. Lin, Y.R. Chang, "Novel Maximum-Power-Extraction Algorithm for PMSG Wind Generation System", *IET Electric Power Applications*, Vol. 1, Issue 2, 2007, pp.275-283.

[6] Y.M. Kawale, S. Dutt, "Comparative Study of Converter Topologies used for PMSG Based Wind Power Generation", *Proc. Int. Conf. on Computer and Electrical Engg.*, Dubai, Vol. 2, Dec. 28-30, 2009, pp. 367-371.

[7] B. Chitti, K.B. Mohanty, "Doubly Fed Induction Generator for Variable Speed Wind Energy Conversion Systems – Modelling and Simulation" *International Journal of Computer and Electrical Engineering*, Vol. 2, No. 1, 2010, pp. 141-147.

[8] LM Fernandez, CA Garcia, F Jurado, "Comparative Study on the Performance of Control Systems for DFIG Wind Turbines Operating with Power Regulation", *Energy 33*, 2008, pp. 1438-1452.

[9] R Pena, JC Clare, GM Asher, "Doubly Fed Induction Generator Using Back to Back PWM Converters and its Application to Variable-Speed Wind-Energy Generation," *IEE Proc. - Electrical Power Applications*, Vol. 143, No. 3, 1996, pp. 231-241.

[10] M. Chinchilla, A. Santiago, C. J. Burgos, "Control of Permanent-Magnet Generators Applied to Variable-Speed Wind-Energy Systems Connected to the Grid", *IEEE Transactions on Energy Conversion*, Vol. 21, No. 1, 2006, pp. 130-135.

[11] A. Rolán, Á. Luna, G. Vázquez, A.Daniel, A. Gustavo, "Modelling of a Variable Speed Wind Turbine with a Permanent Magnet Synchronous Generator", *Proceedings of IEEE International Symposium on Industrial Electronics ISIE*, 2009, pp. 734-739.

[12] A. Khazaee, H.A. Zarchih, M. Ebrahimi, "Robust Maximum Power Point Tracking

Control of Permanent Magnet Synchronous Generator for Grid Connected Wind Turbines", *2nd Iranian Conference on Renewable Energy and Distributed Generation (ICREDG)*, 2012, pp. 75 – 79.

[13] J.G. Slootweg, H. Polinder, W.L. Kling, "Dynamic Modeling of a Wind Turbine with Doubly Fed Induction Generators", *IEEE Power Engg. Society Summer Meeting, Vancouver, BC*, Vol. 1, 2001, pp. 644-649.

[14] D. Liu, J. Hu, C. Zhang, "Blade Design for a Horizontal Axis Variable Speed Wind-Driven Generator", *World Non-Grid-Connected Wind Power and Energy Conf.*, Nanjing, 2009, pp. 1-4.

[15] F.A. Farret, M.G. Simoes, "Integration of Alternative Sources of Energy", *Wiley-IEEE Press (Book)*, 2006.

[16] L. Gidwani, H. Tiwari, "A Comparative Study on the Grid Integrated Wind Energy Conversion Systems Using Different Generator Models" *International Journal of Power and Energy Conversion*, Inderscience Publications, Vol. 3, No. 1/2, 2012.

[17] A. Rolan, A. Luna, G. Vazquez, D. Aguilar, G. Azevedo, "Modeling of a Variable Speed Wind Turbine with a Permanent Magnet Synchronous Generator", *IEEE Int. Symposium on Industrial Electronics*, Seoul, Korea, 2009, pp. 734-739.

[18] S.K. Chung, "Phase-locked Loop for Grid-Connected Three-Phase Power Conversion Systems", *Proc. IEE Electronics Power Applications*, Vol. 147, No. 3, 2000, pp. 213-219.

[19] L. Gidwani, H.P. Tiwari, R.C. Bansal, N. Mithulananthan, "Improving Power Quality of Wind Energy Conversion System With Efficient Power Electronic Interface", *International Journal of Electrical Power and Energy Systems*, Elsevier Publications, 01/2013; 44(1):445-453. DOI:10.1016/j.ijepes.2012.07.051.